Supplementary Materials and Methods

Morpholino knockdown

Morpholino antisense oligonucleotide (MO) was purchased from Gene Tools. The target of *pax1*-MO (5'-CCT CTC CAT AGG TTT GCT CCA TTT G-3') was the sequence at the translation start site of *pax1* mRNA (Mise et al., 2008). As a control experiment, Standard Control MO (5'-CCT CTT ACC TCA GTT ACA ATT TAT A-3') was used, as recommended by Gene Tools. These MOs were dissolved in RNase-free water to a final concentration of 0.5 mM and injected into one-cell-stage embryos.

Skeletal staining

For the visualization of cartilage structures, larvae at 2 days after hatching were fixed overnight in 4% paraformaldehyde at 4°C and then washed two times in phosphate-buffered saline containing 0.1% Tween-20 (PBST). The larvae were stained overnight in alcian blue solution (10% alcian blue, 65% ethanol, 25% glacial acetic acid). After gradual transfer to PBST through an ethanol series, the specimens were bleached with hydrogen peroxide (3% hydrogen peroxide, 1% potassium hydroxide) for 2 hours and washed two times in PBST. Next, the larvae were treated with 1% trypsin in a saturated 30% sodium borate solution at room temperature for 3 hours. Stained larvae were gradually transferred to glycerol. The pharyngeal cartilages were dissected for observation using fine forceps.

TUNEL assay, measurement of the pharynx size and statistics

Apoptotic cells were examined by TUNEL assay. Embryos were fixed with 4% paraformaldehyde overnight at 4°C and then washed three times in PBST. Manually dechorionized embryos were dehydrated with methanol at –20°C. After gradual rehydration, the embryos were permeabilized with 10 µg/ml of proteinase K for 20 minutes at room temperature, followed by 4% paraformaldehyde. After three washes with PBST, the embryos were incubated with 18 µl of labeling solution plus 2 µl of enzyme solution (In Situ Cell Death Detection Kit-TMR Red, Roche) at room temperature for 3 hours. Subsequently, the embryos were washed with PBST three times and stained with DAPI to visualize nuclei and define the endodermal

morphologies. Stained embryos were scanned on an AXIO Imager Z1 with ApoTome (Zeiss). Horizontal Z sections of 1.4-μm thickness, representing a central cross section of the gut tube, were obtained. Within the Z sections, all TUNEL signals distributed in the pharyngeal region posterior to the second arch were counted. The lengths of the pharyngeal regions, from the second pouch to the fifth pouch (in wild type) or the second pouch to the posterior end of the *pax1*-positive endoderm (in *pax1* mutant), were measured on an AXIO Imager Z1 with AxioVision (Zeiss). The mean number of TUNEL-positive cells and mean length of the pharyngeal region were calculated and graphed in Microsoft Excel. Significance was evaluated by a two-tailed Student's *t*-test. Data are presented as mean ± s.e.m., and differences were considered significant at $P < 0.05$.

Mise, T., Iijima, M., Inohaya, K., Kudo, A. and Wada, H. (2008). Function of *Pax1* and *Pax9* in the sclerotome of medaka fish. *Genesis* **46**, 185-192.

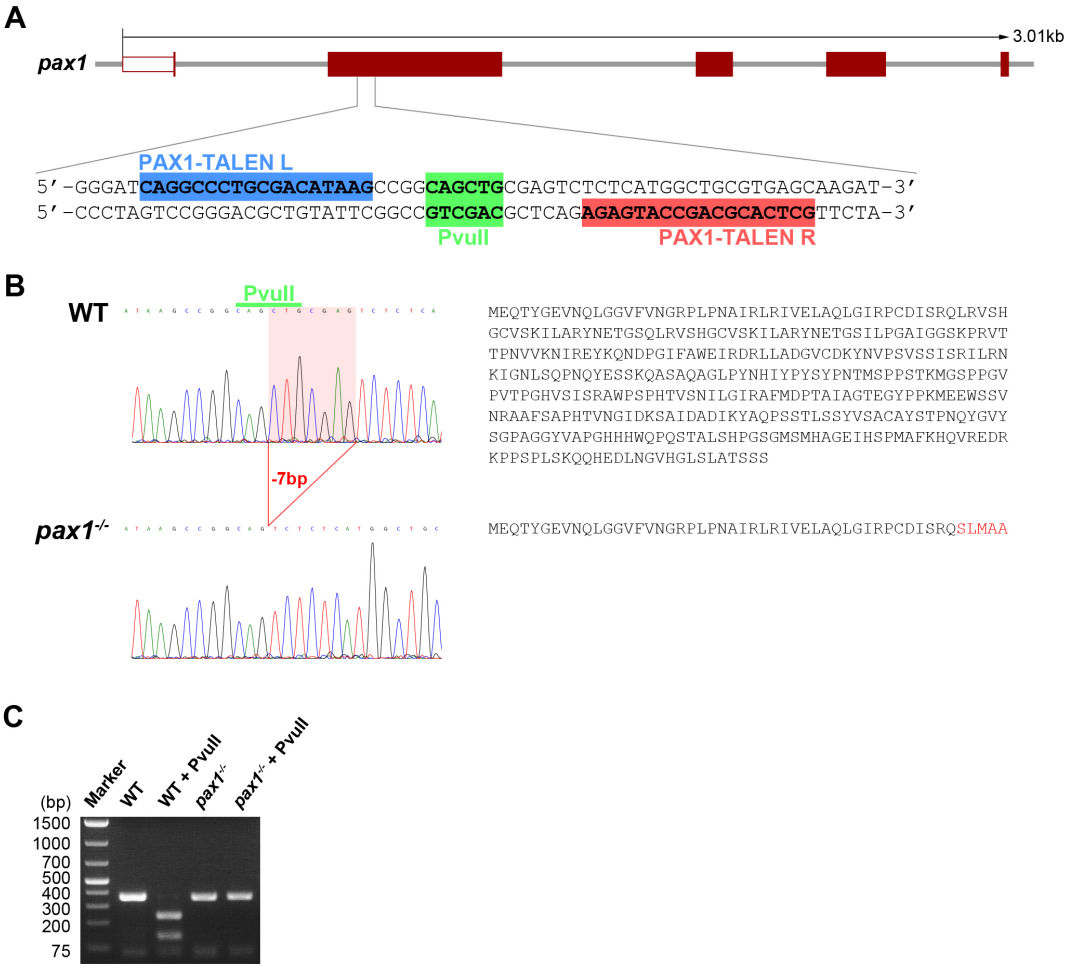

Figure S1. Generation of *pax1* mutants by TALEN.

(A) Schematic representation of the genomic structure of the medaka *pax1* gene and the TALEN target sites. A *Pvu*II restriction site (green) is flanked by the left (blue) and right (red) TALEN target sites in the second exon of *pax1*.

(B) A 7-bp deletion induced by TALEN resulted in significant truncation of the Pax1 protein. Sequencing analysis of the *pax1* mutant showed that the 7-bp deletion contained the *Pvu*II site. This frameshift mutation results in an abnormal amino acid sequence (red SLMAA) and a C-terminal truncation that includes a large part of the paired domain.

(C) Gel image of PCR products for *pax1* genotyping. A fragment of *pax1* was amplified from wild-type and *pax1*-mutant embryos and digested with *Pvu*II, which cleaves the wild-type allele but not the mutant allele. Sequences of the primers for the genotyping were 5’-AGC AAA CCT ATG GAG AGG TG-3’ and 5’-GCT GAT CGA ACT AAC AGA CG-3’.

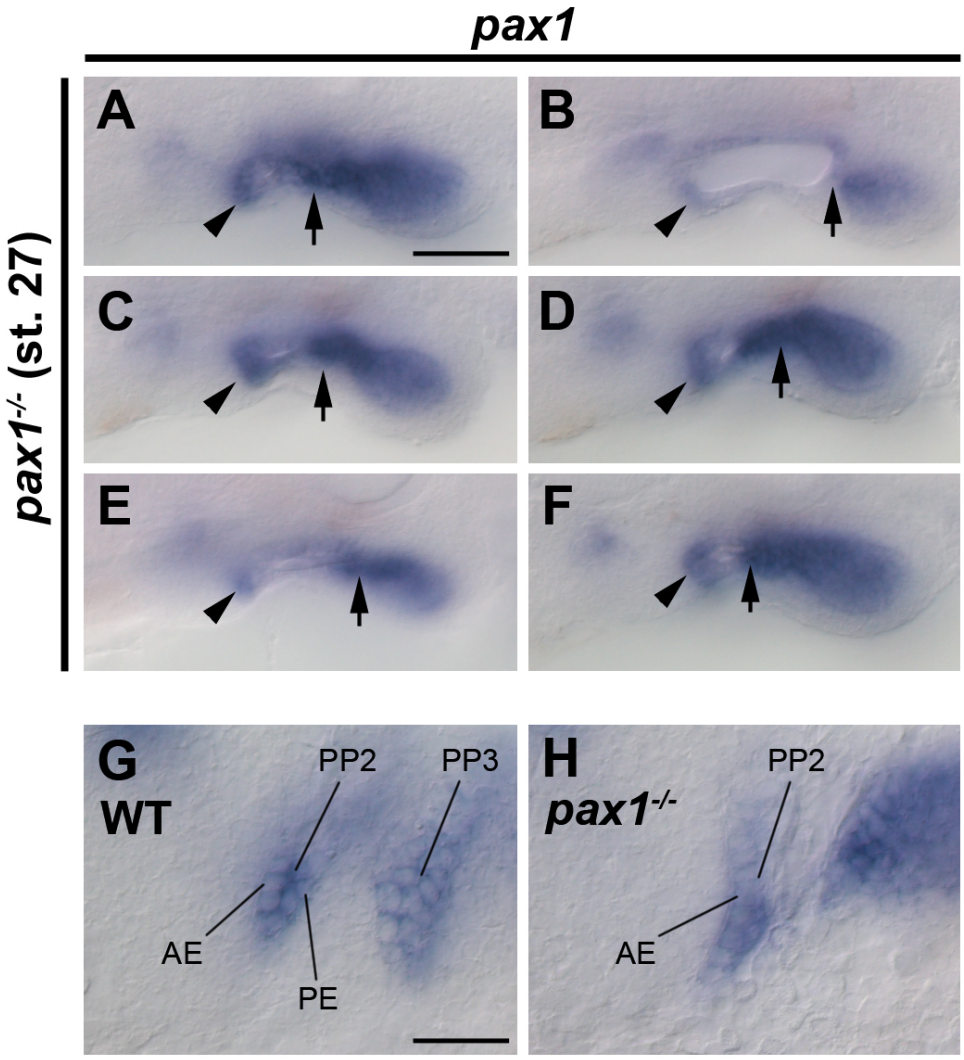

Figure S2. Second pharyngeal pouches in *pax1* mutants.

(A-F) Various morphologies of irregular slits forming posterior to the second arch. The pharyngeal endoderm of *pax1* mutants at stage 27 was visualized using *pax1* expression. Although the positions of the anterior walls of PP2 (arrowheads) were fixed in standard positions, those of the posterior ends of slit openings (arrows) were irregularly set in the mutants.

(G, H) High-magnification flat-mount images focused around PP2 at stage 27. The pharyngeal pouches or endodermal cells were visualized using *pax1* expression. Normally, PP2 (as well as other pouches) exhibited a bilayered morphology, composed of AE and PE. In *pax1* mutants, however, PP2 was composed of monolayer AE, and the PE structure was not found. PP, pharyngeal pouch; AE, anterior epithelium; PE, posterior epithelium. Scale bars, 50 μm in A-F, 25 μm in G and H.

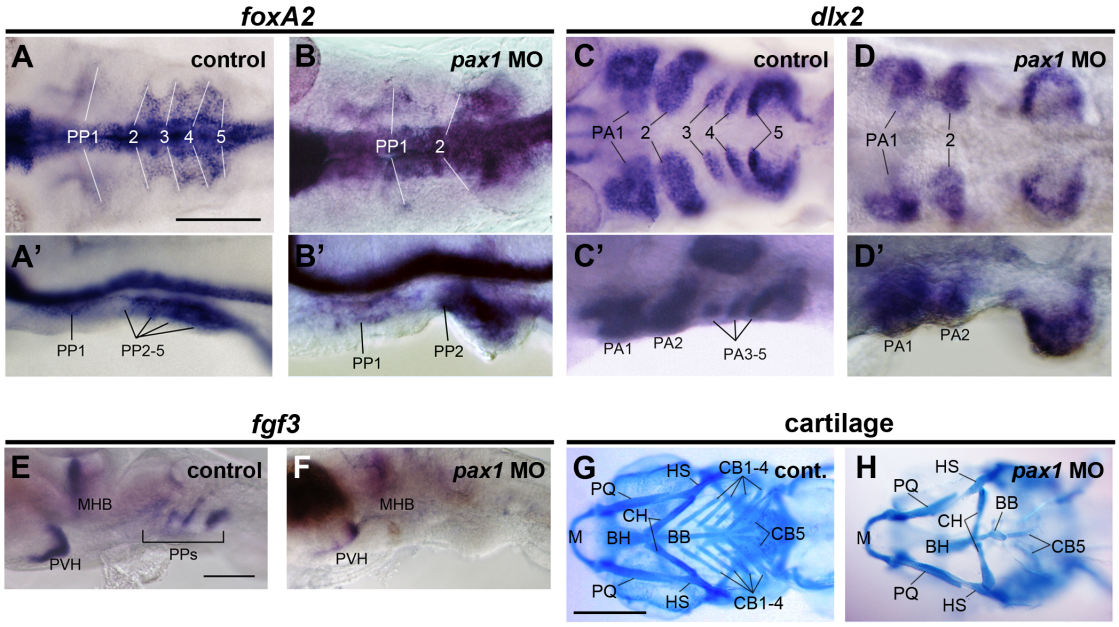

Figure S3. Phenocopy of *pax1* mutants by the *pax1*-specific morpholino.

(A-D) Expression of *foxA2* (A, A', B, B') and *dlx2* (C, C', D, D') was observed at stage 27 to reveal the distribution of neural crest cells and the endoderm, respectively. Whole-mount embryos were observed from the ventral (A-D) and left (A'-D') sides. In *pax1* morphants, although neural crest cells migrated to the ventral side, these cells were not divided into PA3-5 (n = 20/20, D, D') due to defects of PP3-5 (n = 24/27, B, B'), as seen in the *pax1*-mutant embryos.

(D, F) Expression of *fgf3* in control (E) and *pax1* morphant (F) embryos. The pharyngeal expression of *fgf3* was absent in the morphants (n = 8/8, F).

(G, H) Ventral whole-mount views showing alcian blue–stained pharyngeal cartilages of control (G) and *pax1*-morphant (H) larvae at 2 days after hatching. In *pax1* morphants, CB1-4 were lost (n = 18/25, H).

MHB, mid-hindbrain boundary; PA, pharyngeal arch; PP, pharyngeal pouch; PVH, paraventricular hypothalamic nucleus; BB, basibranchial; BH, basihyal; CB, ceratobranchial; CH, ceratohyal; HS, hyosymplectic; M, Meckel's; PQ, palatoquadrate. Scale bars; 100 μm in A and E, 250 μm in G.

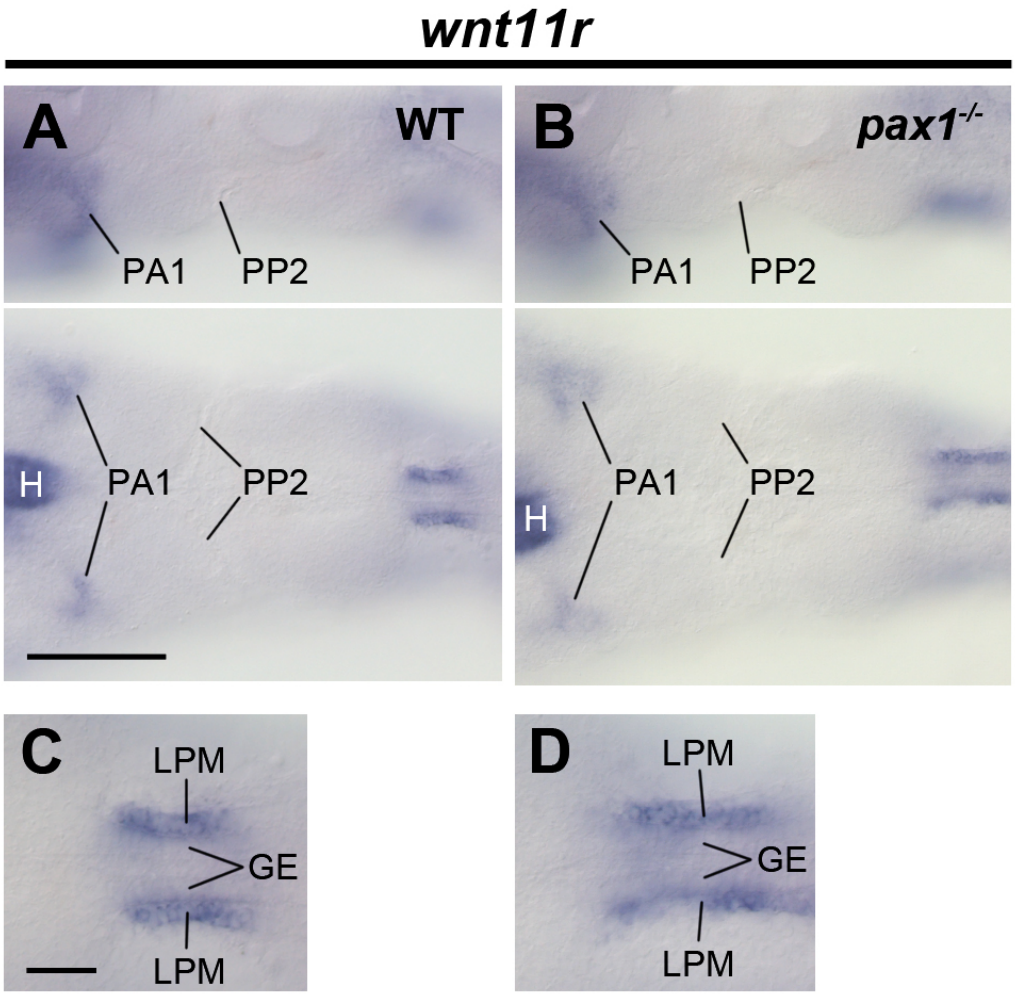

Figure S4. Expression pattern of *wnt11r* in medaka embryos at stage 27.

(A-D) Expression pattern of *wnt11r* in the pharynx of medaka at stage 27. In both wild-type and *pax1*-mutant embryos, *wnt11r* was not expressed in the pharyngeal mesoderm, except for PA1 (n = 19). Mesodermal expression was observed in the LPM surrounding the GE, just posterior to the pharynx, as shown by the high-magnification images of the boundary between the pharynx and the foregut (C, D). In A and B, upper and lower panels show left side and flat-mount views of the embryos, respectively. PA, pharyngeal arch; PP, pharyngeal pouch; LPM, lateral plate mesoderm; GE, gut endoderm. Scale bars: 100 μm in A and B, 25 μm in C and D.

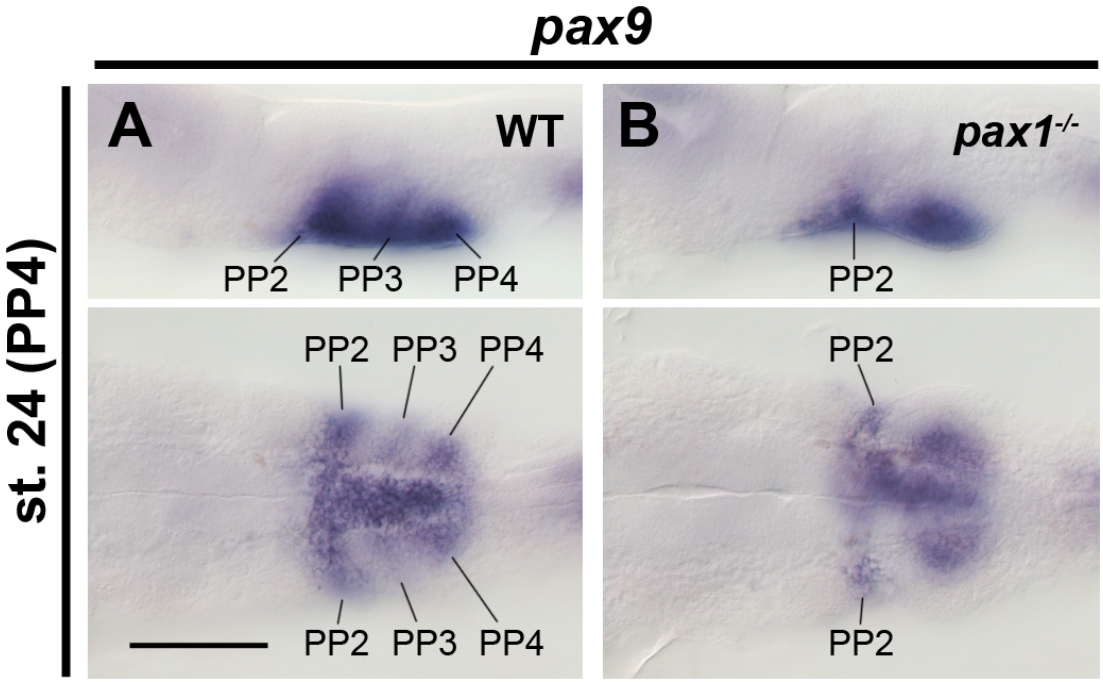

Figure S5. A wide range of *pax9* expression in pharyngeal endoderm.

(A, B) Expression pattern of *pax9* in the pharyngeal endoderm of wild-type (A) and *pax1*-mutant (B) embryos at stage 24. From medial to lateral, *pax9* was widely expressed in the pharyngeal endoderm posterior to the second arch. The *pax9* expression pattern was different from the pouch-specific pattern of *pax1* expression (A). In *pax1* mutants, although the third and fourth pouches were not formed, *pax9* was expressed in the pharyngeal endoderm posterior to the second arch (n = 16, B).

PP, pharyngeal pouch. Scale bar; 100 μm in A.

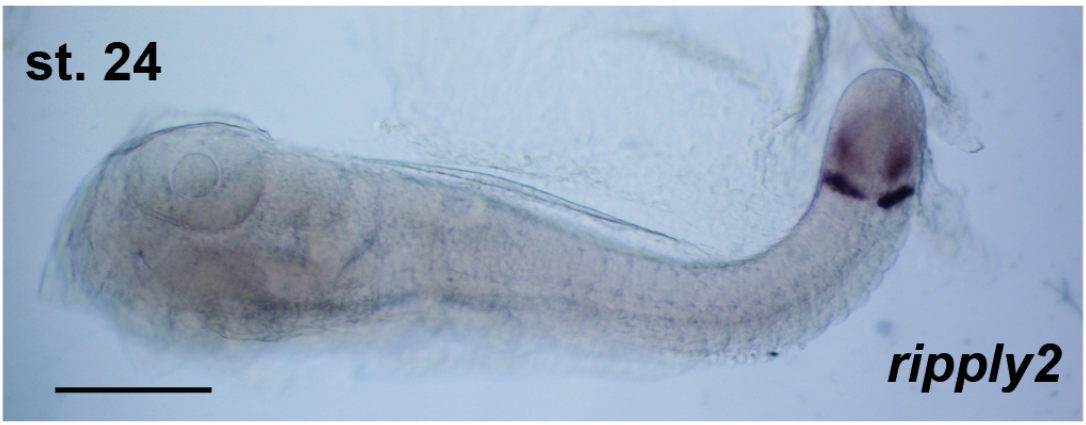

Figure S6. Expression pattern of *ripply2* in the medaka embryo.

The only *ripply* gene in the medaka genome is *ripply2*. At stage 24, expression of *ripply2* was detected in the presomitic mesoderm and in the posterior somites, but not in the pharyngeal region. Scale bar: 200 μm.

Supplementary Tables

Table S1. The list of primers for PCR to amplify cDNA fragments of genes

Gene	Forward primer sequence	Reverse primer sequence
dlx2	5'- GAA CCT AAA CAC CGA TAT GCA TTC CAA CCA -3'	5'- CTA AAA TAT CGT CCC GGC GCT TAT TGC AG -3'
fgf3	5'- CGC TCA GCA TTC ACA CTT TGG ATG G -3'	5'- GCC TCT CTC TTC CTG CCT CGC TTG C -3'
foxA2	5'- GCA GTT AAA ATG GAA GGA CAC GAA CAC AC -3'	5'- GTA GTA GGA TGT GTC GGG TAT AGA TGC AGA -3'
nkx2.3	5'- ACA ATG ATT CCA AGT CCG ATT CTA GCT TCC -3'	5'- TTA CCA TGC CCT GAT CCC CTG CAG AGT TCC -3'
tbx1	5'- ATA CCT ACA ACT ATC CGG GAT CCA ATT CGG -3'	5'- ATT CAT GTG GTG ATG ATA CGT GTG TCC TCT -3'
tcf21	5'- AGT GAG GTT TCC ATG AGC GCA CAG GCG TAT -3'	5'- ATA AAA CAA ACA GGA ACC CGA ATG AAG TAC -3'
ripply2	5'- CAG ACT TTA CGA AGA GCT AAT CAG CGC AAG -3'	5'- CAA TGC TGC TAG TAG AAA TGA GTG CTC TGT -3'
wnt11r	5'- ATG AAG AGC CGC TCT CAC ATC CTG CCT GTT -3'	5'- GGT TGC TGG CAG GAG CAC AGG CCT ATT TGC -3'

Table S2. Defects of pharyngeal cartilages in *pax1* mutants (n=28)

Cartilage phenotype	CB1-4	CB5	CH	HS	PQ	BB
Absent	28	0	0	0	0	0
Shape change	-	9	4	27	2	28
Fusing to other cartilage	-	2 (to BB)	13 (to HS)	13 (to CH), 2 (to PQ)	2 (to HS)	2 (to CB)

BB, basibranchial; CB, ceratobranchial; CH, ceratohyal; HS, hyosymplectic; PQ, palatoquadrate.